

Proposal to detect plane-parallel nodal lines in Sr_2RuO_4 via tunneling spectroscopy

David Parker

U.S. Naval Research Laboratory-Code 6390, 4555 Overlook Avenue SW, Washington D.C. 20375, USA

(Received 23 September 2009; revised manuscript received 6 November 2009; published 28 December 2009)

Since the original proposal of an unconventional chiral order parameter in the ruthenate perovskite superconductor Sr_2RuO_4 , much attention has been given to the possibility of plane-parallel nodal lines on the predominant γ cylindrical Fermi surface given evidence for low-lying quasiparticle excitations in this material. Here I propose a tunneling spectroscopy experiment to determine whether such nodal lines in fact exist.

DOI: 10.1103/PhysRevB.80.220508

PACS number(s): 74.70.-b

I. INTRODUCTION

Superconductivity at approximately 1 K was discovered in Sr_2RuO_4 in 1994 by Maeno *et al.*¹ and since that time has been a topic of strong interest, with substantial experimental and theoretical activity continuing 15 years after its discovery. This material was found following a lengthy search for high-temperature materials structurally similar to the high- T_c cuprates but not containing Cu. It was thought² that a new family of high-temperature superconductors might be discovered in this way, and while this has not happened, interest in this material remains high.

Almost immediately after its discovery, Rice and Sigrist³ proposed that this material contained a two-dimensional p -wave order parameter (OP) as an “electronic analog” to superfluid helium. A closely related compound, SrRuO_3 , shows ferromagnetism, and so the argument was made in analogy to the ferromagnetically mediated pairing in He.

Complicating this simple picture, however, is substantial evidence for nodal excitations in this material. The proposed chiral order parameter would give rise to low-temperature exponentially activated behavior in the various thermodynamic quantities (such as magnetic penetration depth and nuclear-spin-relaxation rate), but this is not what has been observed. Bonalde *et al.*⁴ measured the London penetration depth in single crystals of Sr_2RuO_4 and found a T^2 dependence, while Nishizaki *et al.*⁵ found T^2 specific-heat behavior, evidence for a line-node state. Power-law behavior was also observed in nuclear-spin-relaxation rate (T_1^{-1}) measurements⁶ and ultrasonic attenuation.⁷ In addition, Izawa *et al.*⁸ measured the magnetothermal conductivity of single crystals of Sr_2RuO_4 and found that any nodal lines could not be parallel to the c axis, which immediately suggested $\Delta(\mathbf{k}) = \exp(i\phi)\cos(ck_z)$, given the previous evidence for nodal excitations. The lack of anisotropy in ab -plane magnetothermal conductivity measurements⁹ also suggests any nodal lines are parallel to the basal plane. Most recently, Ishida *et al.*¹⁰ again conducted T_1^{-1} measurements on a high-quality sample of Sr_2RuO_4 and found T^3 behavior, commonly taken as indicative of line nodes. Given these measurements, there may well be nodes parallel to the basal plane on Sr_2RuO_4 .

In this Rapid Communication I propose an experiment that could help determine whether these nodal lines exist. The method is based on tunneling spectroscopy, which can be a strong probe of order-parameter symmetry. The basis of the experiment is presented in Fig. 1 (reprinted from 11), which depicts, in momentum space, an Sr_2RuO_4 c -axis tun-

neling spectroscopy experiment, based upon a recent proposal¹¹ by the author and Thalmeier for the use of graphite as a normal electrode in a superconducting-insulator-graphite tunneling experiment. As the method is described in detail in that publication I only sketch the proposal here. The basic idea is that the use of a gate voltage applied to the semimetal graphite changes the length of the electron-occupied graphite HKH Fermi surface “cigar.” When the graphite is deployed in an appropriate c -axis orientation, as indicated, the conservation of the momentum parallel to the interface k_{\parallel} means that different cigar lengths will sample different regions of the Sr_2RuO_4 Fermi surface. If the superconducting order parameter has no k_z dependence, the sole effect of the lengthening of the cigar will be an increase in conduction channels and thereby merely an overall scale factor in the conductance. However, if the order parameter has k_z dependence, each point on the cigar will see a region of different $\Delta(\mathbf{k})$, producing tunneling or Andreev density of states (DOS) features at that energy. The differential conductance when properly normalized to the high-bias value would thus vary with gate voltage.

In this Rapid Communication I limit myself to a proposal for experimental detection of an $\exp(i\phi)\cos(k_z)$ OP as was originally proposed by Hasegawa *et al.*¹² Several other gap

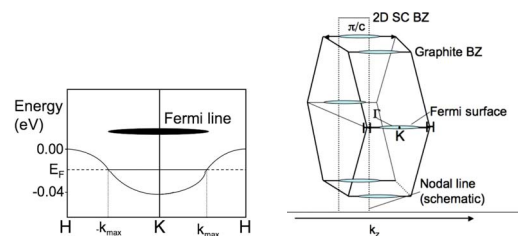


FIG. 1. (Color online) A proposed tunneling spectroscopy experiment between longitudinally oriented graphite and Sr_2RuO_4 (labeled on the right-hand side as 2D SC BZ) to help determine superconducting order-parameter symmetry. On the left is depicted the band structure of graphite between the H and K points with an approximate tight-binding dispersion between these points. Here k_{\max} is the maximum momentum occupied in the ungated situation. On the right, the small blue (gray) cylinders between the H and K points in the right-hand graph are the graphite Fermi surface, which we approximate in the calculations as a line. Depending on the gate-voltage controlled length of the graphite Fermi HK line and assuming parallel momentum conservation between the graphite and superconductor, regions of different order-parameter value are selected by the varying length of the Fermi line, leading to different dI/dV behavior.

functions have been proposed, including the d -wave order parameter $\exp(i\phi)\sin(k_z)$,¹³ as well as various other d -wave and f -wave OPs. The method described herein for the $\exp(i\phi)\cos(k_z)$ will in general yield distinguishable results for any OP with significant k_z dependence but due to space constraints I present explicit results only for this OP.

II. CALCULATION

The calculation presented in this section follows the standard technique applicable to Andreev and tunneling spectroscopy of anisotropic superconducting order parameters^{14–16} and therefore I keep only the most essential details of the calculation. In general, the pair state of a superconductor is described by the Bogoliubov–de Gennes equations:^{14,15,17,18}

$$i\hbar \frac{\partial f}{\partial t} = - \left[\frac{\hbar^2 \nabla^2}{2m} + \mu + V(x) \right] f(\mathbf{x}, \mathbf{k}, t) - \Delta(\mathbf{x}, \mathbf{k}) g(x, t), \quad (1)$$

$$i\hbar \frac{\partial g}{\partial t} = \left[\frac{\hbar^2 \nabla^2}{2m} + \mu + V(x) \right] g(\mathbf{x}, \mathbf{k}, t) - \Delta(\mathbf{x}, \mathbf{k}) f(x, t), \quad (2)$$

with f representing electronlike wave functions and g representing holelike wave functions, with solutions

$$f(\mathbf{x}, \mathbf{k}, t) = u(\mathbf{k}) \exp[i(\mathbf{k} \cdot \mathbf{r} - Et)/\hbar], \quad (3)$$

$$g(\mathbf{x}, \mathbf{k}, t) = v(\mathbf{k}) \exp[i(\mathbf{k} \cdot \mathbf{r} + Et)/\hbar], \quad (4)$$

where u and v are the BCS coherence factors:^{19,20}

$$u(\mathbf{k}) = \sqrt{\frac{1}{2} [1 + \sqrt{E^2 - |\Delta^2(\mathbf{k})|/E}]}, \quad (5)$$

$$v(\mathbf{k}) = \exp(i\phi) \sqrt{\frac{1}{2} [1 - \sqrt{E^2 - |\Delta^2(\mathbf{k})|/E}]}. \quad (6)$$

Here ϕ is the phase of the gap $\Delta(\mathbf{k})$. Given an electron incident from the normal metal, two additional particles result in the metal: an Andreev-reflected hole²¹ and a normally reflected electron, while in the superconductor an electronlike and holelike quasiparticle result. Later in this work we allow for the effect of quasiparticle scattering by letting the energy E have a finite imaginary part Γ .^{16,22–24}

Each of the particles above has a corresponding amplitude (a , b , c , and d , respectively) which is found by specifying the boundary conditions: continuity of the wave function across the boundary, and the following condition applicable to δ -function barrier potentials as introduced in Ref. 14:

$$\psi'_S(0) - \psi'_N(0) = (2m/\hbar^2) H \psi(0), \quad (7)$$

with the barrier function potential $H\delta(x)$ and the effective mass m [we have ignored mass or Fermi velocity mismatch effects as these can be absorbed into the barrier potential Z (Ref. 25)]. Once a and b , the amplitudes for Andreev and normal reflection have been solved for the differential conductance dI/dV is calculated from the following:

$$dI/dV \propto \int dk_{\parallel} [1 + |a(k_{\parallel}, E)|^2 - |b(k_{\parallel}, E)|^2]. \quad (8)$$

The calculated results employ the boundary condition that k_{\parallel} , the momentum parallel to the interface, is conserved. This

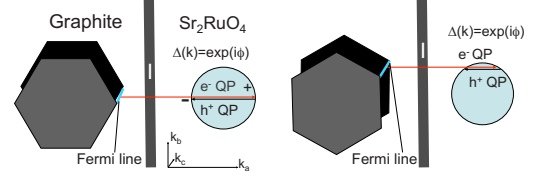


FIG. 2. (Color online) The ab -plane layout of the proposed experiment in momentum space, for two potential graphite orientations. Here the c -axis points into the paper. In each figure, the graphite Brillouin zone is shown on the left, along with its Fermi line, and the Sr_2RuO_4 cylindrical Fermi surface and enclosed area are depicted on the right. For the left figure, since the Fermi line falls at $k_b=0$, perfect Andreev reflection results, while this does not occur for the right figure. Note that the real-space graphite axes are rotated 30° with respect to the momentum space axes. For simplicity, in the right figure and in the calculations we have not accounted for a second Fermi line connecting the H points directly beneath the indicated Fermi line; this line produces very nearly equal conductance, so the effects of this omission are very small.

condition allows for wave vector selection along the longitudinal Sr_2RuO_4 Fermi surface and hence the acquisition of information about the order-parameter value at this wave vector.

We note that for such an ab -plane Sr_2RuO_4 tunneling experiment, the phase of the order parameter is of crucial importance, as it determines the phase of the hole component wave function v . Depicted in Fig. 2 is an ab -plane momentum-space diagram of the proposed experiment in two possible orientations. For the left graph, the electronlike quasiparticle will contact the Sr_2RuO_4 Fermi surface at $k_b=0$, $k_a=k_F$ sampling the order parameter at this wave vector, while the backscattered hole will sample the wave vector directly opposite to this, which introduces a relative phase of -1 among the holelike components of these quasiparticles due to the order-parameter sign change. As shown by Tanaka,¹⁵ such a sign change leads to a zero-bias conductance peak. However, we will see that the character of this peak and surrounding features will depend substantially upon the gate voltage if the order parameter has k_z dependence, leaving a characteristic signature of such a state. On the right is depicted another possible orientation, rotated 30° from the first; for this the perfect Andreev reflection (AR) does not occur and there is no zero-bias enhancement.

III. MAIN RESULT

Depicted in Fig. 3 is the main result of this Rapid Communication. The differential conductance dI/dV is shown in two limits for several gate-induced graphite chemical potential changes for the barrier parameter $Z \equiv H/v_F$: left, $Z=0.3$, corresponding to the point contact regime, and right, $Z=2$, corresponding to the tunneling regime.

Substantial effects of the gating are apparent in both plots. In the top plot, the low-energy Andreev signal evolves from a rounded hump containing a sharp feature at $V=\Delta_0$ toward a nearly linear behavior for $\delta\mu=-12.7$ meV, while in the bottom plot the depression in dI/dV that may sometimes occur adjacent to a ZBCP, most prominent for $\delta\mu=-20$ meV

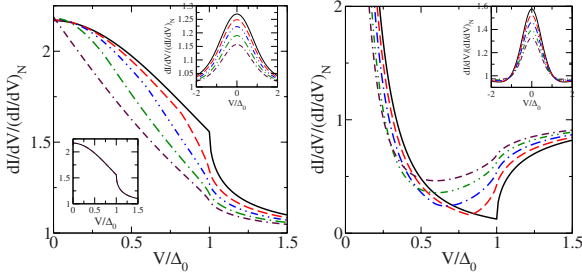


FIG. 3. (Color online) The results of dI/dV calculations in the Andreev limit (left, $Z=0.3$) and tunneling limit (right, $Z=2$), for graphite gated are shown. Dynes Γ taken as zero. Graphite chemical potential changes $\delta\mu = -20$ meV (solid, black), -18.8 meV (dashed, red), -17.3 meV (double-dot-dashed, blue), -15.3 meV (dot-dashed, green) and -12.7 meV (double-dash-dotted, maroon). Top insets: Dynes Γ taken as $0.75\Delta_0$. Bottom inset on left figure: curves (virtually identical) if OP has no k_z dependence.

gradually fills in as the gate voltage increases and lower energy states are accessed, additionally narrowing the peak itself.

The evolution of the curves with gate voltage is easily understood. For the Andreev-limit plot, the width of the AR signal narrows with increasing gate voltage because one is seeing an AR signal from a portion of Fermi surface with smaller $\Delta(\mathbf{k})$ than the maximum gap, and the sharp feature present at $V=\Delta_0$ for $\delta\mu = -20$ meV similarly becomes less prominent. Analogously, for the tunneling limit the width of the ZBCP curves decreases with increasing gate voltage, and the feature at $V=\Delta_0$ is washed out by the summing of ZBCP curves with progressively smaller effective $\Delta(\mathbf{k})$. Note that I have neglected the thickness variation of the “cigar”; inclusion of this effect widens somewhat the range of chemical potential changes over which conductance changes emerge.

These differences are sufficient that a point contact or tunneling experiment performed along these lines should be able to distinguish them. If there is no $\cos(k_z)$ dependence to the order parameter, the dI/dV curves for these varying gate voltages should be essentially identical (up to a scale factor).

For simplicity, we have chosen above the real-space orientation of the graphite such that the hexagonal face parallels the interface. Substantially different dI/dV results obtain if instead the hexagonal face is perpendicular to the interface, as shown in the k space Fig. 2. In this case the 30° rotation of the Brillouin zone relative to the real-space unit cell means that the graphite Fermi lines no longer occur at $k_b=0$, but are displaced above and below by approximately $0.737/\text{\AA}$, which is relatively near the Sr_2RuO_4 γ band k_F of $0.75/\text{\AA}$ so that the perfect order-parameter sign change described above does not occur and one does not see a ZBCP. Results for this case are presented in Fig. 4, for the same parameters as in Fig. 3, and as in the previous plot substantial gate-voltage created differences are apparent, with the Andreev limit peak at $V=\Delta_0$ reducing with increasing gate voltage, while in the tunneling limit substantial sub gap density of states appear with increasing gate voltage.

It is clear that these methods remain applicable even if the k_z dependence of the order parameter is $a+b\cos(k_z)$, with $|a| < b$. The dI/dV curves will still evolve with gate voltage.

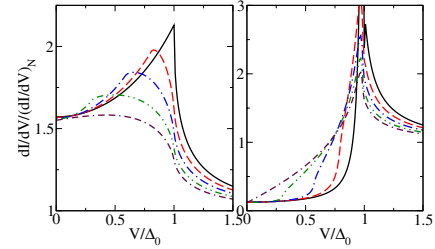


FIG. 4. (Color online) The results of dI/dV calculations in the Andreev limit (left, $Z=0.3$) and tunneling limit (right, $Z=2$), for graphite gated and rotated 30° relative to that of Fig. 3 are shown. Same parameters as in Fig. 3.

The main effect of such a constant term would be to change the gate voltage at which the Fermi-surface cigar accesses the nodal lines, with a minor secondary effect on the shape of the DOS, so long as $a \ll b$.

IV. DISCUSSION

Experimental consideration: surface degradation. The results of the above section suggest that appropriate Andreev or tunneling experiments may be able to determine whether or not there are nodes in the gap function located at $k_z = \pm \pi/2$ as an $\exp(i\phi)\cos(k_z)$ order parameter would contain. There is, however, an experimental consideration requiring consideration: the surface degradation effects in this material.

There are to date four spectroscopic measurements made on Sr_2RuO_4 .^{26,27} The first experiment, by Jin *et al.*,²⁷ performed tunneling on a Pb- Sr_2RuO_4 junction but found only a spectrum strongly resembling that of superconducting lead, with coherence peaks (assumed to be that of Pb) at approximately 1.4 meV and no subgap structure. The second experiment, by Upward *et al.*²⁶ performed c -axis STM using a Pt/Ir tip and found clear evidence of a superconducting gap. The third experiment, by Laube *et al.*,²⁸ observed a weak Andreev reflection signal, as well as a zero-bias anomaly. Of issue for our proposed experiment is the extremely large zero-bias conductance—approximately 0.85 the normal-state value in the Upward *et al.* data. This is believed to result from surface degradation.

A more recent scanning tunneling microscopy (STM) measurement by Suderow *et al.*²⁹ found a fully developed gap, with essentially no subgap conductance and well-developed gap edge peaks of height approximately twice the background conductance. Such a high-quality tunneling measurement suggests that it now may be possible to gather improved data in the Andreev limit as well. Given the several earlier measurements, however, it is important to address the surface issue directly.

A detailed accounting for the possible effects of surface degradation on tunneling or Andreev spectra is rather complicated, particularly as the cause of such degradation remains unknown. Rather than attempt a first principles calculation as such, we therefore content ourselves with two relatively simple mechanisms for simulating the effects of surface degradation.

The first method is empirically based upon the comparative smallness (i.e., relative to background conductance) of the features observed in the early spectroscopic work and the lack of detail in these features. Both of these characteristics are consistent with a large effective “smearing” of the conductance. To a lesser degree, such smearing is nearly universally present in spectroscopy on unconventional superconductors, where it is typically modeled by adding an imaginary part Γ to the quasiparticle energy.²² In fact such a Γ has already been taken to represent the effects of a disordered surface layer.³⁰ Given the predominance of this smearing in experimental spectra of unconventional superconductors and the comparative success of the Dynes Γ in modeling such smearing, it is reasonable to use this parameter to simulate the as-yet-unknown source of surface disorder in Sr_2RuO_4 .

I have performed a calculation, for the graphite orientation used in the main panels of Fig. 3, with a large Dynes Γ of $0.75\Delta_0$; results of this calculation are presented in the insets of Fig. 3. Even with this large Γ , the figures continue to show substantial differences in the dI/dV curves. The zero-bias conductance changes significantly from $\delta\mu = -20$ to -12.7 meV in both the Andreev and tunneling regime as does the shape and size of the Andreev reflection signal so that even if the problems with surface degradation persist, the nodal lines, if existent, will leave their distinctive signature in dI/dV .

A second method of simulating the effects of surface disorder is to relax the assumption of perfect parallel momentum conservation. The premise here is that the surface degradation causes scattering within the interface region so that a finite rather than infinitesimal region of superconductor Fermi surface is allowed to receive current from a given graphite Fermi surface location. In practice one may use a Gaussian distribution of conductance (i.e. $\propto(1+|a|^2 - |b|^2)\exp[-\alpha(k_{\parallel} - k_{0,\parallel})^2]$, where $k_{0,\parallel}$ represents the parallel momentum of the incoming electron and k_{\parallel} represents the parallel momentum of the transmitted quasiparticles) and observe how the dI/dV features change. We note that the boundary conditions of the calculation section do not explicitly involve the parallel momentum so this scheme is inter-

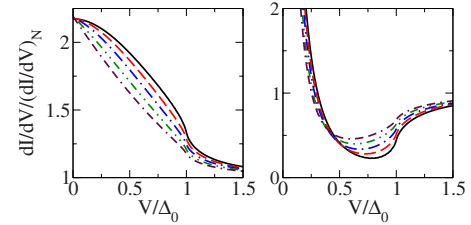


FIG. 5. (Color online) dI/dV curves assuming significant non-conservation of parallel momentum, as described in the text. Same parameters as Fig. 3, top (left here) and bottom (right).

nally consistent. The results are shown in Fig. 5, where we show several Andreev and tunneling limit dI/dV curves assuming an α of $1/\sqrt{0.2\pi}$ (i.e., $\Delta k_{\parallel} \sim 0.2\pi$) in units where 2π is $2\pi/c$ and c is the Sr_2RuO_4 lattice constant of 12.72 \AA . Here δk_{\parallel} is of the same order as typical $k_{\parallel} \sim \pi/2$ so that the non-conservation of parallel momentum is substantial. We have also allowed for nonconservation of k_{\parallel} in the k_b direction, i.e., perpendicular to the graphite Fermi line, and taken account of the $\Delta(\mathbf{k})$ phase factors that result. Even in this case, significant differences in dI/dV remain so that the proposed experiment can be considered robust against the surface degradation issue.

V. CONCLUSION

In this work I have demonstrated that a series of superconductive NIS tunneling measurements on Sr_2RuO_4 using gated graphite as the normal electrode should allow determination of the presence or absence of order-parameter line nodes parallel to the ab -plane. I have shown that the power of such an experiment to determine nodal structure is robust against the surface disorder prevalent in this material. I await the results of such experiments with great interest.

It is a pleasure to acknowledge a valuable discussion with D. J. Van Harlingen and helpful interactions with Y. Tanaka and N. B. Ali. In addition, I wish to thank M. D. Johannes and I. I. Mazin for their reading of this Rapid Communication prior to submission.

¹Y. Maeno *et al.*, Nature (London) **372**, 532 (1994).
²A. P. Mackenzie and Y. Maeno, Rev. Mod. Phys. **75**, 657 (2003).
³T. M. Rice and M. Sigrist, J. Phys.: Condens. Matter **7**, L643 (1995).
⁴I. Bonalde *et al.*, Phys. Rev. Lett. **85**, 4775 (2000).
⁵S. Nishizaki *et al.*, J. Low Temp. Phys. **117**, 1581 (1999).
⁶K. Ishida *et al.*, Phys. Rev. Lett. **84**, 5387 (2000).
⁷C. Lupien *et al.*, Phys. Rev. Lett. **86**, 5986 (2001).
⁸K. Izawa *et al.*, Phys. Rev. Lett. **86**, 2653 (2001).
⁹M. A. Tanatar *et al.*, Phys. Rev. Lett. **86**, 2649 (2001).
¹⁰K. Ishida *et al.*, J. Phys. Chem. Solids **69**, 3108 (2008).
¹¹D. Parker and P. Thalmeier, Phys. Rev. B **76**, 064525 (2007).
¹²Y. Hasegawa *et al.*, J. Phys. Soc. Jpn. **69**, 336 (2000).
¹³I. Zutic and I. I. Mazin, Phys. Rev. Lett. **95**, 217004 (2005).
¹⁴G. E. Blonder *et al.*, Phys. Rev. B **25**, 4515 (1982).
¹⁵Y. Tanaka and S. Kashiwaya, Phys. Rev. Lett. **74**, 3451 (1995).
¹⁶D. Parker and P. Thalmeier, Phys. Rev. B **75**, 184502 (2007).

¹⁷P. G. deGennes, *Superconductivity of Metals and Alloys* (Addison-Wesley, Reading, 1989).
¹⁸T. M. Klapwijk *et al.*, Physica B **109/110**, 1657 (1982).
¹⁹C. Honerkamp and M. Sigrist, J. Low Temp. Phys. **111**, 895 (1998).
²⁰J. R. Schrieffer, *Theory of Superconductivity* (Perseus, Reading, 1999).
²¹A. F. Andreev, Sov. Phys. JETP **19**, 1228 (1964).
²²R. C. Dynes *et al.*, Phys. Rev. Lett. **41**, 1509 (1978).
²³A. Plecenik *et al.*, Phys. Rev. B **49**, 10016 (1994).
²⁴M. Grajcar *et al.*, Phys. Rev. B **51**, 16185 (1995).
²⁵G. E. Blonder and M. Tinkham, Phys. Rev. B **27**, 112 (1983).
²⁶M. D. Upward *et al.*, Phys. Rev. B **65**, 220512(R) (2002).
²⁷R. Jin *et al.*, Phys. Rev. B **59**, 4433 (1999).
²⁸F. Laube *et al.*, J. Low Temp. Phys. **117**, 1575 (1999).
²⁹H. Suderow *et al.*, New J. Phys. **11**, 093004 (2009).
³⁰P. Chalsani, *et al.*, Phys. Rev. B **75**, 094417 (2007).